

Theoretical Bonding Description of Alkylidene Chalcogen (O, S, Se) Difluorides ($\text{H}_2\text{C}=\text{XF}_2$): Planar versus Bent Conformations

J. A. Dobado, Henar Martínez-García, and José Molina Molina*

Grupo de Modelización y Diseño Molecular, Instituto de Biotecnología, Campus Fuentenueva, Universidad de Granada, 18071-Granada, Spain

Received June 23, 1999

Theoretical descriptions of alkylidene chalcogen difluorides have been performed on their planar (1–3) and bent (4–6) conformations. The planar T-shaped conformations were the most stable ones, from the calculations performed (Gaussian-G2 and B3LYP/6-311+G*). The bonding nature of the T-shaped (C_{2v}) structures has also been analyzed by means of the atoms in molecules (AIM) theory and electron localization function analyses.

Introduction

The bonding nature of pnictogen and chalcogen ylides has been controversial for years, and recently Gilheany¹ has reviewed the chemical bonding in phosphine ylides. In this context, our laboratory has performed calculations on pnictogen² and chalcogen³ oxides and sulfides, and very recently a general study on pnictogen and chalcogen ylides has been presented.⁴

Alkylidene chalcogen difluorides present special bonding properties, and the sulfur derivatives were first synthesized by Seppelt et al.⁵ in 1989, and as opposed to the ylide structures they were characterized by a C=S double bond with two different isomers and a large rotational barrier.

In the same work, Seppelt proposed two different conformations for alkylidene sulfur difluoride, a bent conformation with C_s symmetry and a planar T-shaped one with C_{2v} symmetry. Moreover, preliminary HF calculations gave a small energy difference between the two conformers, and the stability order was found to be dependent on the substituents. In addition, the planar T-shaped conformation showed a thiocarbonyl moiety coplanar with a linear F–S–F arrangement. Such kinds of geometrical dispositions (F–S–F linearity) have been postulated experimentally for different alkylidene sulfur tetrafluorides.^{6–11}

The special geometrical arrangement of the F–S bonds for the T-shaped structures and the small energy differences in the

HF calculations warrant further investigation on the potential energy surface for these structures, including a detailed description of the bonding nature. This theoretical bonding description should include the electron correlation effects due to the nature of the F–S–F moiety.

In this paper we present theoretical evidence for the stability of planar T-shaped (C_{2v}) alkylidene chalcogen difluorides together with the topology characterization of the electron charge density, $\rho(r)$, and the electron localization function (ELF). Accurate molecular orbital (MO) calculations have been performed on the two conformers of the title compounds (1–6) presented in Figure 1.

Computational Details

(a) General Methods. Density functional theory (B3LYP) and Gaussian-G2¹² calculations were performed with the Gaussian 98 package of programs.¹³ All the structures were fully optimized at the B3LYP/6-311+G* level, with constrained C_{2v} or C_s symmetry, and tested with frequency calculations (no imaginary frequencies). The Bader analysis has been done with the AIMPAC series of programs,¹⁴ using the DFT density as input as was described in the atoms in molecules (AIM) theory.^{15,16} The $\nabla^2\rho(r)$ and ELF contour-map representations have been produced using the MORPHY98 program.¹⁷ The atomic charges have been calculated with use of the AIMPAC

* To whom correspondence should be addressed. E-mail: jmolina@ugr.es.

- (1) Gilheany, D. G. *Chem. Rev.* **1994**, *94*, 1339.
- (2) Dobado, J. A.; Martínez-García, H.; Molina, J. Sundberg, M. R. *J. Am. Chem. Soc.* **1998**, *120*, 8461.
- (3) Dobado, J. A.; Martínez-García, H.; Molina, J. Sundberg, M. R. *J. Am. Chem. Soc.* **1999**, *121*, 3156.
- (4) Dobado, J. A.; Martínez-García, H.; Molina, J. Sundberg, M. R. *J. Am. Chem. Soc.*, in press.
- (5) Damerius, R.; Seppelt, K.; Thrasher, J. S. *Angew. Chem., Int. Ed. Engl.* **1989**, *28*, 769.
- (6) Seppelt, K. *Angew. Chem., Int. Ed. Engl.* **1990**, *30*, 361.
- (7) Bock, H.; Boggs, J. E.; Kleemann, G.; Lentz, D.; Oberhammer, H.; Peters, E. M.; Seppelt, K.; Simon, A.; Solouki, B. *Angew. Chem., Int. Ed. Engl.* **1979**, *18*, 944.
- (8) Krügerke, T.; Buschmann, J.; Kleemann, G.; Luger, P.; Seppelt, K. *Angew. Chem., Int. Ed. Engl.* **1987**, *26*, 799.
- (9) Buschmann, J.; Koritsanszky, T.; Kuschel, R.; Luger, P.; Seppelt, K. *J. Am. Chem. Soc.* **1991**, *113*, 233.
- (10) Buschmann, J.; Damerius, R.; Gerhardt, R.; Lentz, D.; Luger, P.; Marschall, R.; Preugschat, D.; Seppelt, K. Simon, A. *J. Am. Chem. Soc.* **1992**, *114*, 9465.
- (11) Kuschel, R.; Seppelt, K. *Inorg. Chem.* **1993**, *32*, 3568.

- (12) Curtiss, L. A.; Raghavachari, K.; Trucks, G. W.; Pople, J. A. *J. Chem. Phys.* **1991**, *94*, 7221.
- (13) Gaussian 98, revision A.4: M. J. Frisch, G. W. Trucks, H. B. Schlegel, G. E. Scuseria, M. A. Robb, J. R. Cheeseman, V. G. Zakrzewski, J. A. Montgomery, Jr., R. E. Stratmann, J. C. Burant, S. Dapprich, J. M. Millam, A. D. Daniels, K. N. Kudin, M. C. Strain, O. Farkas, J. Tomasi, V. Barone, M. Cossi, R. Cammi, B. Mennucci, C. Pomelli, C. Adamo, S. Clifford, J. Ochterski, G. A. Petersson, P. Y. Ayala, Q. Cui, K. Morokuma, D. K. Malick, A. D. Rabuck, K. Raghavachari, J. B. Foresman, J. Cioslowski, J. V. Ortiz, B. B. Stefanov, G. Liu, A. Liashenko, P. Piskorz, I. Komaromi, R. Gomperts, R. L. Martin, D. J. Fox, T. Keith, M. A. Al-Laham, C. Y. Peng, A. Nanayakkara, C. Gonzalez, M. Challacombe, P. M. W. Gill, B. Johnson, W. Chen, M. W. Wong, J. L. Andres, C. Gonzalez, M. Head-Gordon, E. S. Replogle, and J. A. Pople, Gaussian, Inc., Pittsburgh, PA, 1998.
- (14) Biegler-König, F. W.; Bader, R. F. W.; Tang, T.-H. *J. Comput. Chem.* **1982**, *3*, 317.
- (15) Bader, R. F. W. *Atoms in Molecules: a Quantum Theory*; Clarendon Press: Oxford, 1990.
- (16) Bader, R. F. W. *Chem. Rev.* **1991**, *91*, 893.
- (17) MORPHY98: a program written by P. L. A. Popelier with a contribution from R. G. A. Bone, UMIST, Manchester, England, EU, 1998.

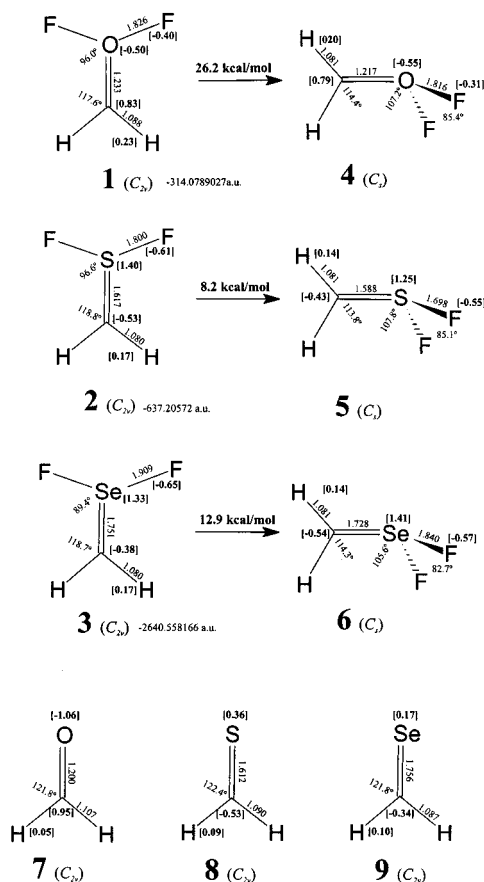


Figure 1. Alkyldiene chalcogen (O, S, Se) difluoride $\text{H}_2\text{C}=\text{XF}_2$ structures **1–6** and related parent compounds **7–9** (symmetry in parentheses), together with the geometrical parameters, atomic charges (in brackets), and total and relative energies calculated at the B3LYP/6-311+G**/B3LYP/6-311+G* level.

series of programs,¹⁴ by integration over the basin of every atom in the Bader framework.

(b) Overview of the $\rho(r)$ and ELF Topologies. The topology of the electronic charge density, $\rho(r)$, as pointed out by Bader,¹⁵ is an accurate mapping of the chemical concepts of atom, bond, and structure. The principal topological properties are summarized in terms of their critical points (CPs).^{15,16} The nuclear positions behave topologically as local maxima in $\rho(r)$. A bond critical point (BCP) is found between each pair of nuclei, which are considered to be linked by a chemical bond, with two negative curvatures (λ_1 and λ_2) and one positive curvature (λ_3) (denoted as (3, -1) CP). The ellipticity, ϵ , of a bond is defined by means of the two negative curvatures in a BCP as

$$\epsilon = \lambda_1/\lambda_2 - 1 \quad \text{where} \quad |\lambda_2| < |\lambda_1| \quad (1)$$

The ring CPs are characterized by a single negative curvature. Each (3, -1) CP generates a pair of gradient paths¹⁵ which originate at a CP and terminate at neighboring attractors. This gradient path defines a line through the charge distribution linking the neighboring nuclei. Along this line, $\rho(r)$ is a maximum with respect to any neighboring line. Such a line is referred to as an atomic interaction line.^{15,16} The presence of an atomic interaction line in such equilibrium geometry satisfies both the necessary and sufficient conditions that the atoms be bonded together.

The Laplacian of the electronic charge density, $\nabla^2\rho(r)$, describes two extreme situations. In the first $\rho(r)$ is locally concentrated ($\nabla^2\rho(r) < 0$), and in the second it is locally depleted ($\nabla^2\rho(r) > 0$). Thus, a value of $\nabla^2\rho(r) < 0$ at a BCP is unambiguously related to a covalent bond, showing that a sharing of charge has taken place. While in a closed-shell interaction, a value of $\nabla^2\rho(r) > 0$ is expected, as found in noble gas repulsive states, ionic bonds, hydrogen bonds, and van der Waals molecules. Bader has also defined a local electronic energy

density, $E_d(r)$, as a functional of the first-order density matrix:

$$E_d(r) = G(r) + V(r) \quad (2)$$

where $G(r)$ and $V(r)$ correspond to local kinetic and potential energy densities, respectively.¹⁵ The sign of $E_d(r)$ determines whether accumulation of charge at a given point r is stabilizing ($E_d(r) < 0$) or destabilizing ($E_d(r) > 0$). Thus, a value of $E_d(r) < 0$ at a BCP presents a significant covalent contribution and, therefore, a lowering of the potential energy associated with the concentration of charge between the nuclei.

The ELF function,^{18,19} which was first introduced by Becke and Edgecombe,²⁰ can be viewed as a local measure of the Pauli repulsion between electrons due to the exclusion principle, allowing us to define regions of space that are associated with different electron pairs. The ELF function is expressed by

$$\text{ELF} = 1/[1 + (D/D_h)^2] \quad (3)$$

where

$$D = \frac{1}{2} \sum_{j=1}^N |\nabla\varphi_j|^2 - \frac{1}{8} \frac{|\nabla\rho|^2}{\rho}$$

$$D_h = (3/10)(3\pi^2)^{2/3} \rho^{5/3} \quad (4)$$

$$\rho = \sum_{j=1}^N |\varphi_j|^2$$

This definition gives ELF values between 0 and 1, with large values where two antiparallel spin electrons are paired in space; on the contrary, this value is small in the regions between electron pairs.

Results and Discussion

Calculations have been performed on both conformations of methylene sulfur difluoride and on the corresponding chalcogen derivatives (structures **1–6**; see Figure 1).

Density functional theory (B3LYP) calculations, which include electron correlation, have been done using the high-quality 6-311+G* basis set. The results are summarized in Figure 1. All the calculations showed the T-shaped conformers to be the most stable ones, compared to the bent C_s ones (26.2, 8.2, and 12.9 kcal/mol for **1**, **2**, and **3**, respectively).

The bent structures (**4–6**) present a disposition on the X atoms (O, S, and Se) which is almost tetrahedral, with the plane formed by the CH_2 bisecting the F–S–F angle. All the general geometrical features (planarity of the CH_2 subunit, short CX bond lengths, and almost trigonal bond angles at the C atom) were compatible with the existence of a $\text{C}=\text{X}$ double bond. The $\text{C}=\text{X}$ bond distances showed noticeable characteristics; for **4**, this bond length was larger than in formaldehyde. However, these double bonds for **5** and **6** were shorter than those of their corresponding parent compounds **8** and **9** (1.588 and 1.728 Å vs 1.612 and 1.756 Å, respectively), showing $\text{C}=\text{X}$ bond stabilization.⁶

The planar T-shaped structures have a $\text{H}_2\text{C}=\text{X}$ moiety very close to those of the corresponding carbonyl analogues (**7**, **8**, and **9**), with a F–X–F lineal arrangement in the same plane, compatible with $\angle\text{F–X–C}$ angles close to 90° (96.0° , 90.6° , and 89.4° for **1**, **2**, and **3**, respectively). The XF bonds were longer than standard single XF bonds,³ in

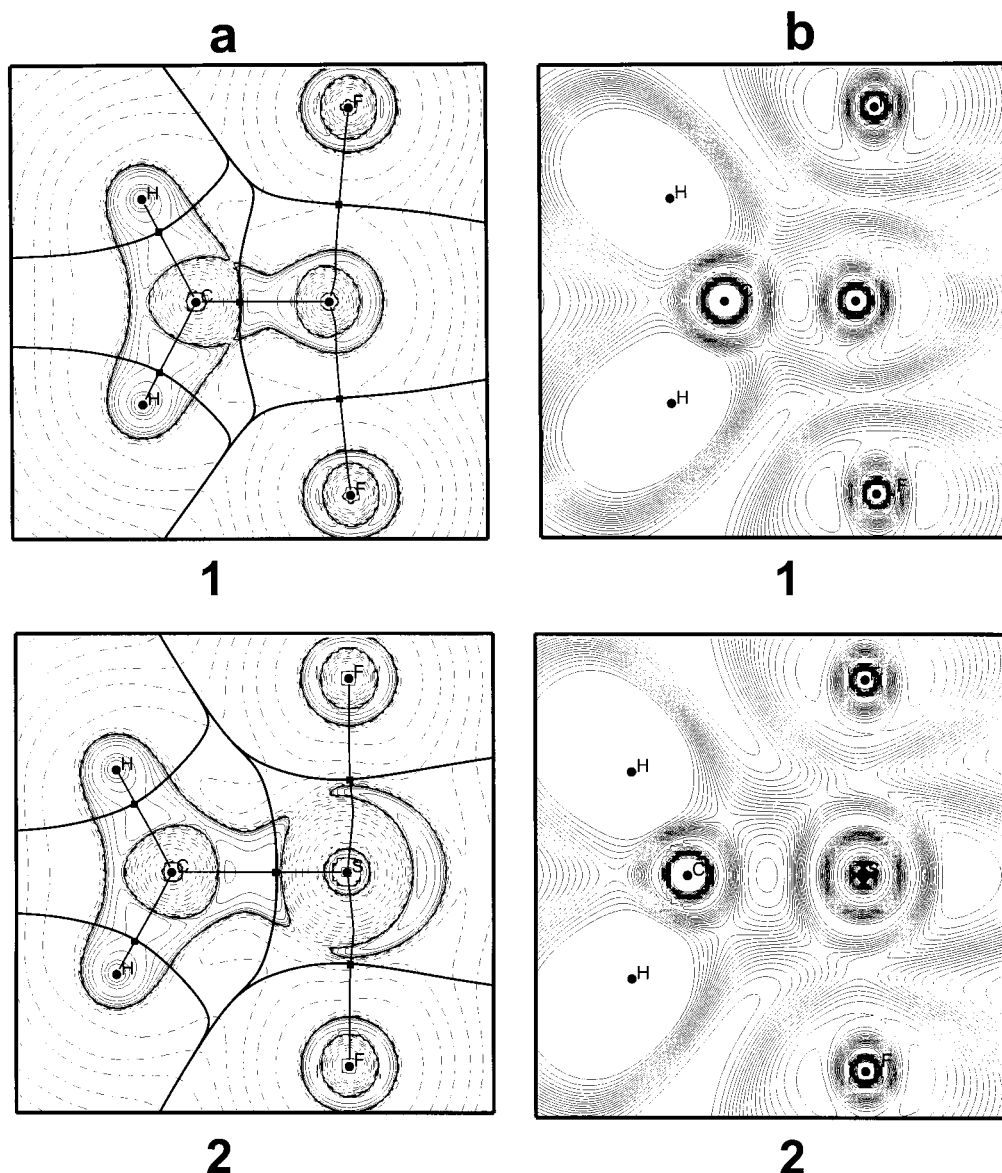
(18) Silvi, B.; Savin, A. *Nature* **1982**, *371*, 683.

(19) Bader, R. F. W.; Johnson, S.; Tang, T.-H.; Popelier, P. L. A. *J. Phys. Chem.* **1996**, *100*, 15398.

(20) Becke, A. D.; Edgecombe, K. E. *J. Chem. Phys.* **1990**, *92*, 5397.

Table 1. Charge Density, $\rho(r)$, Laplacian of the Charge Density, $\nabla^2\rho(r)$, Ellipticity, ϵ , and Electronic Energy Density, $E_d(r)$, for the BCPs of 1–9 and XF₂ Related Structures, at the B3LYP/6-311+G**/B3LYP/6-311+G* Theoretical Level

structure	$\rho(r)$ (e/a_0^3)	$\nabla^2\rho(r)$ (e/a_0^5)	ϵ	$E_d(r)$	structure	$\rho(r)$ (e/a_0^3)	$\nabla^2\rho(r)$ (e/a_0^5)	ϵ	$E_d(r)$
(1) H ₂ C=OF ₂					(4) H ₂ C=OF ₂				
C–O	0.380	0.167	0.081	–0.613	C–O	0.386	0.499	0.068	–0.619
O–F	0.092	0.422	0.001	0.007	O–F	0.092	0.423	0.019	0.008
(2) H ₂ C=SF ₂					(5) H ₂ C=SF ₂				
C–S	0.262	–0.520	0.765	–0.351	C–S	0.271	–0.680	0.458	–0.280
S–F	0.132	0.092	0.061	–0.069	S–F	0.166	–0.082	0.033	–0.133
(3) H ₂ C=SeF ₂					(6) H ₂ C=SeF ₂				
C–Se	0.206	–0.166	0.403	–0.162	C–Se	0.211	–0.204	0.377	–0.168
Se–F	0.108	0.279	0.047	–0.033	Se–F	0.128	0.283	0.014	–0.050
(7) H ₂ C=O					OF ₂				
C–O	0.414	0.080	0.040	–0.696	O–F	0.291	0.304	0.094	–0.179
(8) H ₂ C=S					SF ₂				
C–S	0.240	–0.107	0.045	–0.302	S–F	0.177	0.000	0.568	–0.172
(9) H ₂ C=Se					SeF ₂				
C–Se	0.193	–0.047	0.128	–0.146	Se–F	0.137	0.344	0.195	–0.060

**Figure 2.** $\nabla^2\rho(r)$ (a) and ELF (b) contour maps, in the molecular plane for structures 1 and 2 at the B3LYP/6-311+G* level. The $\nabla^2\rho(r)$ contours begin at zero and increase (dashed contours) and decrease (solid contours) in steps of ± 0.02 , ± 0.04 , ± 0.08 , ± 0.2 , ± 0.4 , ± 0.8 , ± 2.0 , ± 4.0 , and ± 8.0 . The thick solid lines represent the molecular graph that joins the nuclei (solid circles) and the BCP (solid squares), and also the zero flux surface. The ELF contours range from 0 to 1 and increase in steps of 0.02.

particular for structure 1. The differences were ca. 0.42, 0.16, and 0.12 Å for 1–3, respectively.

The T-shaped special disposition resembles those found for the fluorine axial substituents in methylene sulfur tetrafluoride

compounds.^{6,21} However, the lack of additional equatorial fluorine atoms for **1–3** gave noticeable geometrical features which deserve to be reviewed.

The theoretical level used (B3LYP/6-311+G*/B3LYP/6-311+G*) has proved its ability to describe related hypervalent compounds.^{2,3} In addition, the geometric features have also been tested at a higher level (CCSD/6-311G*/CCSD/6-311G*), yielding similar geometrical parameters for **1**. Moreover, the stability order, obtained at the B3LYP level, has been carefully tested by performing Gaussian-G2 calculations¹² on structures **2** and **5**, and the results stabilized structure **2** in 3.7 kcal/mol (G2 energy $-636.397\ 551$ hartrees for **2**).

The electronic analysis and that for the bond nature on the T-shaped planar structures (**1–3**) have been performed using the “atoms in molecules” theory^{15,16} and electron localization function.^{18,19,22} The bonding schemes for the X=CH₂ subunits resemble those of their corresponding parent compounds **7–9**, and two different situations were described. First, structure **1** showed very small differences with respect to formaldehyde itself (positive $\nabla^2\rho(r)$ values and small ϵ values). However, the C–X BCPs for **2** and **3** increased for the $\rho(r)$, $-\nabla^2\rho(r)$ and ϵ values, showing a larger electron charge concentration in the X–C bond, together with a multiple bond character reinforcement. Moreover, the $E_d(r)$ values were larger and negative, for **1–3**. All the above were compatible with the proposed S=C double-bond stabilization experimentally detected for the related compounds.⁶

On the other hand, the bonding scheme for the F–X–F subunits is defined as follows: the F–X bonding region is mainly a positive $\nabla^2\rho(r)$ one. In addition, the F–X BCPs presented very low $\rho(r)$ values, and smaller than did the standard X–F single bonds. The $\nabla^2\rho(r)$ values were all positive and the $E_d(r)$ ones low or even positive, compatible with a closed-shell type of interaction. However, the F–X bond length deviations, from the standard single bonds, were larger in **1** than in **2** or **3**, in agreement with the numerical BCP values (see Table 1).

Furthermore, the calculated Bader atomic charges supported all the previous considerations (see Figure 1). For **1**, the charges on the O and C atoms were smaller than the corresponding ones in the formaldehyde molecule, yielding a weaker electrostatic interaction. The opposite was found for **2** and **3**, in which the charges on the C atom were similar to those in **8** and **9**, while the charges on X atoms were larger. The charges on the O and F atoms were both negative, explaining by means of electrostatic repulsions the longer F–O bond. However, for **2** and **3**, the F and X atoms had opposite charges, giving bonds closer to the

standard X–F single bonds despite the special geometrical arrangement. Also, the charges on both F atoms were large and negative for **1–3**.

The overall description of the bonding nature was made by analyzing the $\nabla^2\rho(r)$ and ELF topologies. In Figure 2, contour maps of $\nabla^2\rho(r)$ and ELF were depicted for **1** and **2**, together with their corresponding bond path lines and the interatomic surfaces. The representations for **3** were completely similar to those for **2**.

There is charge concentration along the C–X bond (negative $\nabla^2\rho(r)$ region), and the $\nabla^2\rho(r)$ contour maps for the H₂C=X subunit were very similar to those of the formaldehyde molecule.²³ The main difference between **1** and **2** was that the electronic charge concentration along the C–X bond belongs to the O atom for **1**, and on the contrary to the C atom for **2**, as is compatible with the calculated charges.

Both representations showed electronic charge depletion along the F–X bonds, indicating a closed-shell type of interaction. Furthermore, an additional lone pair, on the X atoms, was located pointing away from X and along the C–X axis. The existence of only two maxima in $-\nabla^2\rho(r)$, located along the C–X axis, was also confirmed numerically.

The ELF representations confirmed the above bonding scheme. The bonding attractors in the C–X bond belong to the O atom in **1**, and to the C atom in **2**. There is also an additional nonbonded attractor (electron pair) along the C–X bond. However, there were no attractors along the F–X bond path, and a deep valley was located in the F–X BCP.

Conclusions

Calculations on both planar and bent alkylidene chalcogen difluorides showed the planar structures as the preferred ones, at the B3LYP/6-311+G* level for structures **1–3**. In addition, the planar structure **2** was also the most stable at the G-2 level.

The overall bonding nature described above, the molecular graphs displayed (T-shaped arrangement), the $\nabla^2\rho(r)$ and ELF topological analyses, and the calculated atomic charges on F and X atoms all agreed with a three-center four-electron bond^{24,25} for the F–X–F arrangement.

Acknowledgment. Computing time was provided by the Universidad de Granada. We are grateful to Professor R. F. W. Bader for a copy of the AIMPAC package of programs. We thank David Nesbitt for reviewing the language of the manuscript.

IC9907330

(21) Xie, Y.; Schaefer, H. F.; Thrasher, J. S. *THEOCHEM: J. Mol. Struct.* **1991**, *80*, 247.

(22) Savin, A.; Nesper, R.; Wengert, S.; Fässler, T. *Angew. Chem., Int. Ed. Engl.* **1997**, *36*, 1808.

(23) See ref 12, p 313.

(24) Pimentel, G. C. *J. Chem. Phys.* **1951**, *19*, 446.

(25) Hach, R. J.; Rundle, R. E. *J. Am. Chem. Soc.* **1951**, *73*, 4321.